Journal of Thermal Analysis and Calorimetry, Vol. 62 (2000) 665–679

MIXED LIGAND COMPLEXES OF 5-ARYLAZO-8-HYDROXYQUINOLINE AND α–AMINO ACIDS WITH Co(II), Ni(II) AND Cu(II)

A. S. A. Zidan, A. I. El-Said, M. S. El-Meligy, A. A. M. Aly and O. F. Mohammed

Chemistry Department, Faculty of Science, Assiut University, Assiut, Egypt

(Received April 17, 2000)

Abstract

Ten mixed ligand complexes of the type [M(X-QA)(aa)] and [Ni(X-QA)$_2$(Haa)(H$_2$O)], where *X-HQA*= 5-arylazo-8-hydroxyquinoline derivatives, *M*=Co(II) or Cu(II) and *Haa*=glycine (gly), alanine (ala) or methionine (met), have been prepared. The complexes have been characterized by elemental analysis, IR and electron spectra and thermal analysis. A tetrahedral structure has been proposed for the cobalt(II) and copper(II) complexes with bidentate coordination of amino acids. The nickel(II) complexes have been assigned an octahedral structure with the amino acids acting as monodentate ligands. The thermal behaviour of the complexes has been studied before and after γ-irradiation.

Keywords: α-amino acids, 5-arylazo-8-hydroxyquinoline, characterization, mixed ligand complexes, thermal analysis

Introduction

Azo compounds are known to be involved in a number of biological reactions such as inhibition of DNA, RNA and protein synthesis, carcinogenesis and nitrogen fixation [1–3]. Furthermore they are proved to have biological activity against bacteria and fungi [4–5]. Some of the 8-hydroxyquinoline derivatives and their complexes with transition metals were reported to be active *vs*. bacteria [6]. In view of the above importance of azo and 8-hydroxyquinoline compounds and the biological significance of amino acids, a number

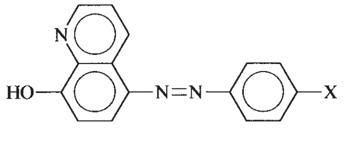

5-(arylazo-8-hydroxyquinoline)

X=H or CH$_3$

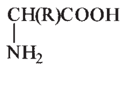

$\underset{NH_2}{CH(R)COOH}$

R=H, CH$_3$, or CH$_3$SCH$_2$CH$_2$-
α-amino acids

1418–2874/2000/ $ 5.00

Akadémiai Kiadó, Budapest
Kluwer Academic Publishers, Dordrecht

of mixed ligand complexes of Co(II), Ni(II) and Cu(II) with some α-amino acids and substituted 5-arylazo-8-hydroxyquinoline were prepared and characterized.

Experimental

All reagents and solvents required for the preparation of the compounds were of AR grade and used without purification. All metal chlorides were obtained from Merck and α-amino acids were purchased from BDH. The substituted 5-arylazo-8-hydroxyquinolines were prepared by published procedure [7].

Preparation of the ternary complexes

The following general procedure was adopted for the synthesis of the ternary complex. 5-Phenylazo-8-hydroxyquinoline or 5-(*p*-methyl-phenylazo)-8-hydroxyquinoline (5 mmol) in 50 ml ethanol was added with stirring to 2.5 mmol of metal chloride in 20 ml aqueous ethanolic solution, when a solution (20 ml) of 2.5 mmol of α-amino acid was added an orange to brown precipitates formed were filtered, washed with ethanol and dried over P_4O_{10}.

Physical measurements

The infrared spectra were recorded on a 470 Shimadzu infrared spectrophotometer. The electron absorption spectral measurements were carried out on a UV-2101PC Shimadzu spectrophotometer. The thermogravimetric analyses were determined by using an electrobalance of the type Sartorius 200MP converted to a thermobalance by the addition of a small furnace and sample holder. The temperature was measured by using a Chromel-Alumel thermocouple attached to a digital multimeter type Soar ME-550, the heating rate was adjusted to be 8°C $\min^{-1}$. The complexes were kept in small glass containers and subjected to γ-irradiation for appropriate times at ambient temperature by using a ^{60}Co gamma cell having a dose rate of 1.1 Gy s^{-1}.

Results and discussion

The complexes are partially soluble in ethanol and acetone; they have good solubility in DMSO. Analytical data, decomposition points and colours of the complexes are shown in Table 1.

Mixed ligand complexes are easily formed according to the following equations:

$$\mathrm{Haa+M^{2+}+X\text{-}HQA \rightarrow [M(X\text{-}QA)(aa)]+2H^+} \qquad (1)$$

$$\mathrm{Haa+Ni^{2+}+2(X\text{-}HQA) \xrightarrow{H_2O} [Ni(X\text{-}QA)_2(Haa)(H_2O)]+2H^+} \qquad (2)$$

where *M*=Co(II) or Cu(II) *X-HQA*=5-phenylazo-8-hydroxyquinoline (HQA) or 5-*p*-methyl-phenylazo-8-hydroxyquinoline (*p*-Me-HQA) and *Haa*=glycine (gly), alanine (ala) or methionine (met). As can be seen from Eqs 1 and 2, the Co(II) and Cu(II) complexes are formed in the molar ratios 1:1:1 (metal ion:X-QA^-:aa^-), while

Table 1 Colour, elemental analyses and decomposition temperature of the complexes

Compound	Colour	Elemental analysis/%								Decomp. *m.p.*/°C
		C		H		N		M		
		found	calcd.	found	calcd.	found	calcd.	found	calcd.	
[Co(*p*-Me-QA)(gly)]	brown	54.71	54.69	4.02	4.08	14.22	14.17	14.79	14.91	309
[Co(*p*-Me-QA)(ala)]	brown	55.70	55.76	4.77	4.43	13.68	13.68	14.40	14.39	303
[Ni(QA)$_2$(Hgly)(H$_2$O)]	orange	59.35	59.28	4.22	4.20	14.89	15.12	9.12	9.06	337
[Ni(QA)$_2$(Hala)(H$_2$O)]	pale orange	59.71	59.84	4.46	4.41	14.79	14.80	8.90	8.86	332
[Ni(QA)$_2$(Hmet)(H$_2$O)]	orange	58.17	58.18	4.62	4.60	13.61	13.57	8.14	8.13	327
[Ni(*p*-Me-QA)$_2$(Hgly)(H$_2$O)]	pale orange	60.55	60.38	4.66	4.62	14.51	14.49	8.76	8.68	327
[Ni(*p*-Me-QA)$_2$(Hala)(H$_2$O)]	pale orange	60.97	60.89	4.83	4.82	14.20	14.20	8.50	8.50	322
[Ni(*p*-Me-QA)$_2$(Hmet(H$_2$O)]	orange	59.42	59.21	5.02	4.97	13.12	13.05	7.92	7.82	319
[Cu(*p*-Me-QA)(gly)]	reddish brown	54.02	54.06	4.00	4.03	14.09	14.01	15.81	15.89	269
[Cu(*p*-Me-QA)(ala)]	reddish brown	55.22	55.13	4.66	4.38	13.59	13.53	15.44	15.35	255

the Ni(II) complexes possess the molar ratio 1:2:1. The complexes were obtained by mixing the metal ion and the two ligands in the molar ratio 1:2:1.

IR spectra

The most important IR peaks of the complexes are reported in Table 2. Mixed ligand complexes exhibit the characteristic bands of the involved ligands. Thus, the 5-arylazo-8-hydroxyquinoline moieties display three bands in the regions 1380–1410, 1550–1570 and 1130–1140 cm^{-1} corresponding to ν(N=N), ν(C=N) and ν(C–O), respectively. The position of ν(C=N) and ν(C–O) indicates that the coordination occurs through nitrogen and oxygen of the 8-hydroxyquinoline part [8, 9] for all the complexes.

The free amino acids exhibit $\nu_s(NH_2)$ around 3120 cm^{-1} [10–13]. The band is shifted to lower frequency region ($\Delta\nu$=20–80 cm^{-1}) in the spectra of the complexes, indicating the involvement of the amino nitrogen in coordination. For the complexes [Co(*p*-Me-QA)(gly)], [Co(*p*-Me-QA)(ala), [Cu(*p*-Me-QA)(gly)] and [Cu(*p*-Me-QA)(ala)], the bands due to $\nu(COO^-)$ of carboxylic group are observed in the region 1570–1575 cm^{-1}; a lowering of the frequency of this band suggests the coordination of the carboxylic oxygen to the metal ions.

The IR spectra of $[Ni(QA)_2(Hgly)(H_2O)]$, $[Ni(QA)_2(Hala)(H_2O)]$, $[Ni(QA)_2(Hmet)(H_2O)]$, $[Ni(p\text{-Me-QA})_2(Hgly)(H_2O)]$, $[Ni(p\text{-Me-QA})_2(Hala)(H_2O)]$ and $[Ni(p\text{-Me-QA})_2(Hmet)(H_2O)]$ display a band in the region 1590–1600 cm^{-1}, this band can be assigned to ν(COOH). Furthermore, the ν(OH) stretching vibrations of coordinated water are located in the region 3300–3400 cm^{-1}.

From the forgoing band positions of $\nu(NH_2)$, $\nu(COO^-)$ and comparison with similar compounds [14], it may be concluded that the amino acids in the complexes Co(II) and Cu(II) are bidentate coordinating through the NH_2 and COO^- groups and monodentate through the NH_2 group in the Ni(II) complexes. Monodentate coordinate ion of amino acids is known in the literature [15, 16]. For all the complexes, metal–nitrogen and metal–oxygen bonds are manifested by the appearance of two bands in the ranges 415–428 and 460–480 cm^{-1}, respectively. This is further evidence for coordination of the metal ions through oxygen and nitrogen atoms of the ligands.

The electron spectra

The electron spectral data of the complexes in DMSO and Nujol mull are given in Table 3. For the Co(II) and Cu(II) complexes, a relatively intense band is observed in the region 450–480 nm, which can be attributed to the characteristic azo $n\rightarrow\pi^*$ [9, 17]. The complexes further display a band in the range 388–417 nm; this band is assigned to charge transfer transition (most probably LMCT). It seems that the *d-d* transitions of both Co(II) and Cu(II) complexes are obscured by the azo group absorption in the expected *d–d* regions. The close similarity between the electron spectra of the complexes and related compounds [18] indicates the tetrahedral structure around Co(II) and Cu(II). For the Ni(II) complexes, however, a *d–d* band appears in the range 500–601 nm, due to the transition $^3A_{2g}(F)\rightarrow{}^3T_{1g}(F)$ (ν_2) typical of octahedral

Table 2 IR absorption bands of the complexes

Compound	ν(N=N)	ν(C=N)	ν(C–O)	ν(C–N)	ν(COOH)	ν(COO^-)	ν(NH_2)	ν(OH)	ν(M–O)	ν(M–N)
[Co(*p*-Me-QA)(gly)]	1390	1570	1135	1490	–	1575	3050	–	465	420
[Co(*p*-Me-QA)(ala)]	1400	1570	1140	1500	–	1570	3050	–	470	420
[Ni$(QA)_2$(Hgly)(H_2O)]	1400	1560	1135	1498	1590	–	3050	3350	460	420
[Ni$(QA)_2$(Hala)(H_2O)]	1410	1565	1140	1500	1590	–	3100	3400	465	425
[Ni$(QA)_2$(Hmet)(H_2O)]	1400	1550	1130	1495	1600	–	3050	3400	460	428
[Ni(*p*-Me-QA)$_2$(Hgly)(H_2O)]	1400	1560	1140	1490	1595	–	3040	3300	480	420
[Ni(*p*-Me-QA)$_2$(Hala)(H_2O)]	1405	1555	1135	1490	1600	–	3100	3350	460	420
[Ni(*p*-Me-QA)$_2$(Hmet)(H_2O)]	1405	1560	1135	1490	1600	–	3050	3380	460	415
[Cu(*p*-Me-QA)(gly)]	1380	1570	1130	1495	–	1570	3100	–	460	425
[Cu(*p*-Me-QA)(ala)]	1380	1565	1140	1490	–	1575	3050	–	465	425

structure around Ni(II). The transition ν_3 is obscured by the band of the azo group located in the region 457–477 nm. The charge transfer transition of the nickel(II) complexes occurs in the range 355–408 nm. For all the complexes, the bands at 258–279 nm are associated with intraligand transitions.

Table 3 Electron spectral bands for the complexes λ_{max} (nm)

Complex	In DMSO	In Nujol
[Co(*p*-Me-QA)(gly)]	480, 410, 258	453, 417, 279
[Co(*p*-Me-QA)(ala)]	479, 411, 260	470, 410, 271
[Ni(QA)$_2$(Hgly)(H$_2$O)]	500, 359, 265	503, 462, 408, 258
[Ni(QA)$_2$(Hala)(H$_2$O)]	504, 370, 266	510, 471, 403, 260
[Ni(QA)$_2$(Hmet)(H$_2$O)]	507, 375, 266	539, 477, 376
[Ni(*p*-Me-QA)$_2$(Hgly)(H$_2$O)]	500, 355, 270	500, 453, 355, 279
[Ni(*p*-Me-QA)$_2$(Hala)(H$_2$O)]	506, 356, 270	560, 455, 358
[Ni(*p*-Me-QA)$_2$(Hmet)(H$_2$O)]	502, 360, 260	601, 473, 373
[Cu(*p*-Me-QA)(gly)]	456, 266	460, 450, 388, 359, 276
[Cu(*p*-Me-QA)(ala)]	457, 267	451, 392, 360, 276

From the forgoing data the following structures can be postulated.

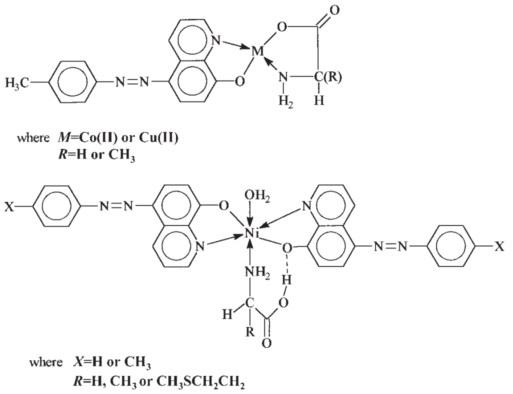

Fig. 1 Suggested structure for the complexes

Thermal analysis

The thermogravimetric analysis of the complexes were recorded in the 50–600°C range. The complexes [Co(*p*-Me-QA)(gly)] and [Co(*p*-Me-QA)(ala)] show the same decomposition pattern. They decompose in two steps at 136, 135 and 382 and 375°C (DTG curves), respectively. The first step is related to the evolution of a nitrogen molecule (found 6.8 and 6.5%; calc. 7.0 and 6.7%) respectively leaving compound (I) (Eq. (3) which decomposes in the second step. The final product is CoO. Elimination

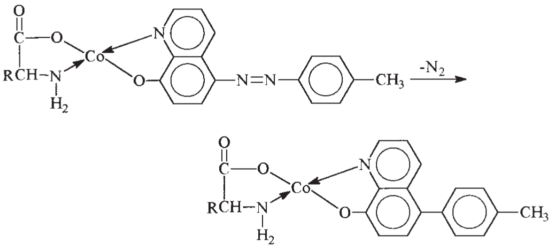

(I)

(3)

of nitrogen molecule from metal complexes of 5-arylazo-8-hydroxyquinoline during their thermal decomposition is known in the literature [8].

Table 4 Thermal data of the complexes

Complex	Step	T_i/	T_m/ °C	T_f/	Mass loss (calcd.)/%
[Co(*p*-Me-QA)(gly)]	1st 2nd	130 300	136 382	151 451	6.8 (7.0) 74.7 (–)
[Co(*p*-Me-QA)(ala)]	1st 2nd	130 294	135 375	145 444	6.5 (6.7) 73.8 (–)
[Ni(QA)$_2$(Hgly)(H$_2$O)]	1st 2nd	122 331	140 398	169 456	7.3 (7.1) 80.9 (–)
[Ni(QA)$_2$(Hala)(H$_2$O)]	1st 2nd	119 325	138 390	166 450	7.1 (6.9) 81.8 (–)
[Ni(QA)$_2$(Hmet)(H$_2$O)]	1st 2nd	116 319	150 388	180 450	6.4 (6.2) 82.6 (–)
[Ni(*p*-Me-QA)$_2$(Hgly)(H$_2$O)]	1st 2nd	120 319	140 405	177 505	6.5 (6.6) 81.7 (–)
[Ni(*p*-Me-QA)$_2$(Hala)(H$_2$O)]	1st 2nd	115 327	131 390	160 451	6.3 (6.5) 82.6 (–)
[Ni(*p*-Me-QA)$_2$(Hmet)(H$_2$O)]	1st 2nd	105 350	124 428	160 500	6.1 (6.0) 83.8 (–)
[Cu(*p*-Me-QA)(gly)]	1st 2nd 3rd	– 341 582	265 466 596	– 542 615	28.8 45.9 5.8
[Cu(*p*-Me-QA)(ala)]	1st 2nd 3rd	– 338 572	261 452 589	– 536 610	27.3 47.6 5.4

The TG curves of the Ni(II) complexes, [Ni(QA)$_2$(Hgly)(H$_2$O)], [Ni(QA)$_2$(Hala)(H$_2$O)], [Ni(QA)$_2$(Hmet)(H$_2$O)], [Ni(*p*-Me-QA)$_2$(Hgly)(H$_2$O)], [Ni(*p*-Me-QA)$_2$(Hala)(H$_2$O)] and [Ni(*p*-MeQA)$_2$(Hmet)(H$_2$O)] consist of two stages of mass loss. The first mass loss occurs in the range 124–150°C and can be attributed to a loss of one water and one nitrogen molecules. The second step is a major step in the TG curve of all the complexes and corresponds to unidentified decomposition products. The final product for these complexes is the NiO.

Three decomposition steps are observed in the TG curves of [Cu(*p*-Me-QA(gly)] and [Cu(*p*-Me-QA)(ala)]. It was difficult to correlate the first and the second decomposition steps of the two complexes with the proper decomposition products. However, the third step in both complexes at 596 and 589°C respectively, is consistent with the formation of $CuCO_3$, which decomposes to the final product CuO.

Kinetic parameters of the complexes

The Coast–Redfern [19] and Horowitz–Metzger [20] equations were used for evaluating the kinetic parameters.

- Coats–Redfern equation

$$\ln\left[\frac{1-(1-\alpha)^{1-n}}{(1-n)T^2}\right]=\frac{M}{T}+B \text{ for } n\neq 1 \tag{4}$$

$$\ln\left[\frac{-\ln(1-\alpha)}{T^2}\right]=\frac{M}{T}+B \text{ for } n=1 \tag{5}$$

where $M=-E/R$ and $B=\ln ZR/\phi E$ where E, R, Z and ϕ are the activation energy, gas constant, pre-exponential factor and heating rate, respectively.

- Horowitz–Metzger equation

$$\ln\left[\frac{1-(1-\alpha)^{1-n}}{1-n}\right]=\ln\frac{ZRT_s^2}{\phi E}-\frac{E}{RT_s}+\frac{E\theta}{RT_s^2} \text{ for } n\neq 1 \tag{6}$$

$$\ln[-\ln(1-\alpha)]=\frac{E\theta}{RT_s^2} \text{ for } n=1 \tag{7}$$

where $\theta=T-T_s$ is the temperature at the DTG peak.

The correlation coefficient *r* was computed by using the least square method for Eqs (4), (5), (6) and (7). Linear curves were drawn for different values of *n* ranging from 0 to 2 in increments of 0.2. The value of *n*, which gave the best fit, was chosen as the order parameter for the decomposition stage of interest. The kinetic parameters were calculated from the plots of the L.H.S. of Eqs (4) and (5) *vs.* $1/T$ and *vs.* θ for Eqs (6) and (7) (Figs 2 and 3).

For all the complexes studied, the activation energies of the first and second steps are recorded in Table 5. The activation energies for the elimination of nitrogen molecule from the cobalt(II) complexes are shown in the range 41.9–48 kJ mol^{-1}. Regarding the nickel(II) complexes, the activation energy of the first step is shown in the range 71.9–91.9 kJ mol^{-1}. Moreover, the copper(II) complexes exhibit an activation energy of 94.4–104.1 kJ mol^{-1} for the first step.

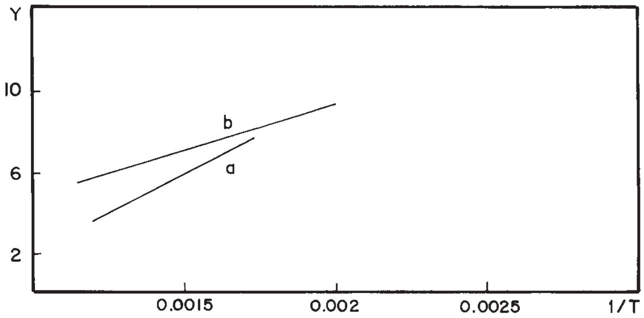

Fig. 2 Coats–Redfern plots for the two decomposition steps of [Cu(p-Me-QA)(gly)]; a – first step; b – second step where $Y=\ln\{[1-(1-\alpha)^{1-n}]/[(1-n)T^2]\}$ for $n\neq1$ or $Y=\ln[-\ln(1-\alpha)]$ for $n=1$

Table 5 Kinetic parameters of the complexes

Complexes	Step	Coats–Redfern			Horowitz–Metzger		
		n	r	E/ kJ mol^{-1}	n	r	E/ kJ mol^{-1}
[Co(p-Me-QA)(gly]	1st	0.00	1.000	48	0.00	0.998	50.00
	2nd	2.00	0.998	280	2.00	0.995	290.90
[Co(p-Me-QA)(ala)]	1st	0.00	0.989	41.9	0.00	0.999	45.80
	2nd	2.00	0.990	380	2.00	0.997	369.80
[Ni(QA)$_2$(Hgly)(H$_2$O)]	1st	1.00	0.987	91.9	0.33	0.994	87.17
	2nd	2.00	0.992	113	2.00	1.000	120.00
[Ni(QA)$_2$(Hala)(H$_2$O)]	1st	1.00	0.999	79.42	1.00	0.996	83.13
	2nd	0.66	0.979	163	0.66	0.999	171.22
[Ni(QA)$_2$(Hmet)(H$_2$O)]	1st	1.00	1.000	72.15	1.00	0.999	75.21
	2nd	2.00	0.992	–	2.00	0.995	131.60
[Ni(p-Me-QA)$_2$(Hgly)(H$_2$O)]	1st	1.00	0.999	84.9	1.00	0.996	79.60
	2nd	0.66	0.995	109.2	0.66	0.999	102.80
[Ni(p-Me-QA)$_2$(Hala)(H$_2$O)]	1st	0.66	1.000	71.9	2.00	0.997	–
	2nd	0.66	0.989	188.1	0.66	0.996	190.20
[Ni(p-Me-QA)$_2$(Hmet)(H$_2$O)]	1st	1.00	0.995	79.95	1.00	0.998	75.62
	2nd	1.00	0.996	108.7	1.00	0.997	110.72
[Cu(p-Me-QA)(gly)]	1st	–	–	–	–	–	–
	2nd	2.00	0.994	104.1	2.00	0.999	107.78
	3rd	0.00	0.996	196.1	0.00	0.977	202.72
[Cu(p-Me-QA)(ala)]	1st	–	–	–	–	–	–
	2nd	2.00	0.991	94.43	2.00	0.997	99.22
	3rd	0.33	1.000	165.9	0.00	0.999	–

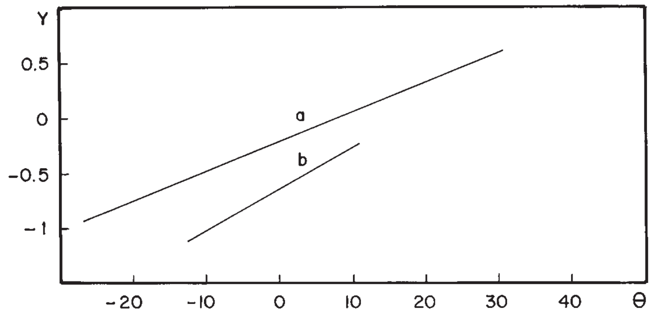

Fig. 3 Horowitz–Metzger plots for the two decomposition steps of $[Ni(p\text{-}Me\text{-}QA)_2(Hmet)(H_2O)]$; a – first step; b – second step where $Y=\ln[(1-(1-\alpha)^{1-n})/(1-n)]$ for $n\neq1$ or $Y=\ln[-\ln(1-\alpha)]$ for $n=1$

Thermal studies of irradiated samples

Four complexes were selected for irradiation with γ-rays at doses of 10^4 and 10^5 Gy. These complexes are $[Co(p\text{-}Me\text{-}QA)(gly)]$, $[Ni(QA)_2(Hmet)(H_2O)]$, $[Ni(p\text{-}Me\text{-}QA)_2(Hgly)(H_2O)]$ and $[Cu(p\text{-}Me\text{-}QA)(gly)]$. The irradiated samples exhibit essentially the same TG profile compared to those before irradiation (Fig. 4). Table 6 includes the initial temperature (T_i), peak temperature (T_m) and final temperature (T_f) of decomposition after irradiation. The cobalt(II) and copper(II) complexes are most affected by the two γ-ray doses among the studied complexes. Thus, irradiation of the cobalt(II) complex lowers T_m by 9 and 21°C of the first step and by 15 and 26°C of the second step, upon irradiation with the 10^4 and 10^5 Gy doses, respectively. For the copper(II) complex, irradiation with the 10^4 and 10^5 Gy doses lowers T_m of the first step by 10 and 25°C, of the second step by 10 and 19°C and of the third step by 19 and 28°C. The Ni(II) complexes are practically unaffected by the two doses at 10^4 and 10^5 Gy.

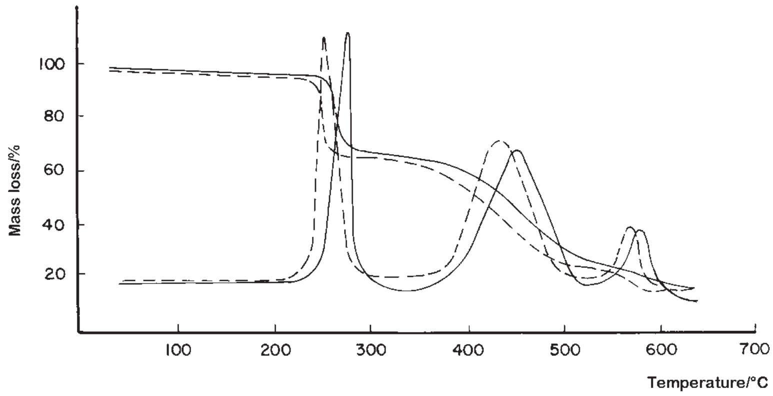

Fig. 4 TG and DTG curves of unirradiated (—) and γ-irradiated (---) $[Cu(p\text{-}Me\text{-}QA)(gly)]$. Irradiation dose=$1\cdot10^5$ Gy

Table 6 Thermal data after γ-irradiation of 10^4 and 10^5 Gy

Compound	Step	Irradiaton dose: 10^4 Gy			Irradiation dose: 10^5 Gy		
		T_i/	T_m/	T_f/	T_i/	T_m/	T_f/
		°C					
[Co(*p*-Me-QA)(gly)]	1st	120	127	145	112	115	137
	2nd	292	367	440	287	356	430
[Ni(QA)$_2$(Hmet)(H$_2$O]	1st	116	146	177	114	141	172
	nd	317	382	441	313	376	438
[Ni(*p*-Me-QA)$_2$(Hgly)(H$_2$O)]	1st	117	135	164	114	132	161
	2nd	313	387	447	323	380	445
[Cu(*p*-Me-QA)(gly)]	1st	–	255	–	–	240	–
	2nd	335	436	535	323	427	524
	3rd	571	587	607	560	558	590

The activation energy of the different decomposition steps was calculated by using the Coats–Redfern and Horowitz–Metzger equations. Table 7 shows that the activation energy of the irradiated complexes decreases compared with the unirradiated ones. The two Co(II) and Cu(II) complexes display a greater decrease in activation energy than those of the Ni(II) complexes. This may suggest their lower stability besides the autocatalytic effect of Co(II) and Cu(II) on the decomposition of their complexes. However, there are relatively small changes in activation energy for all the studied complexes by increasing the radiation dose, suggesting that the same chemical processes govern the decomposition of the complexes for the two doses. The influence of γ-irradiation on the thermal decomposition of [Cu(*p*-Me-QA)(gly)] is depicted in Fig. 4.

The IR spectra of the irradiated [Co(*p*-Me-QA)(gly)] and [Cu(*p*-Me-QA)(gly)] complexes (Figs 5 and 6) show that the intensity of most of the bands decreases and that the metal oxygen (460–480 cm^{-1}) or metal nitrogen (415–428 cm^{-1}) bands are more affected with irradiation. However, the position of all the bands did not change with irradiation. As expected from the thermal decomposition data of Co(II), Ni(II) and Cu(II) complexes, the effect of Co(II) and Cu(II) complexes are more pronounced, whereas those of Ni(II) experience no change upon irradiation. The degradation mechanism of the M–O and M–N bands is suggested as follows. The γ-ray ionizes the complex to produce positive ions and electrons. The excited unstable ions then decompose by bond scission to give uncharged complex molecule and metal cations. These cations are then neutralized through recombination with the slowed-down electrons to form metallic atoms [21]. In conclusion, it is evident that γ-irradiation leads to the rupture of some metal oxygen and metal nitrogen bonds and hence results in a decrease of the intensity of the IR band of the M–O or M–N bonds.

Antibacterial activity

The data listed in Table 8 indicate that the Ni(II) complexes are inactive against the tested bacteria (except against *B. cereus* G+ve), whereas the two complexes of Co(II) and

Table 7 Kinetic parameters of the decomposition of complexes after irradiation with 10^4 and 10^5 Gy irradiation doses

Complex	Step	Coats–Redfern				Horowitz–Metzger			
		n	r	E_1	E_2	n	r	E_1	E_2
[Co(p-Me-QA)(gly)]	1st	0.00	1.000	41.2	33.52	0.00	0.998	44	36.0
	2nd	2.00	0.998	266	251.5	2.00	0.995	275	252.5
[Ni(QA)$_2$(Hmet)(H$_2$O)]	1st	1.00	0.999	70.0	66.21	1.00	0.999	71	68.5
	2nd	2.00	0.979	–	–	2.00	0.995	128	124.12
[Ni(p-Me-QA)$_2$(Hgly)(H$_2$O)]	1st	1.00	0.999	84	78.0	1.00	0.996	70.2	67.9
	2nd	0.66	0.995	100	92.5	0.66	0.999	93.2	88.5
[Cu(p-Me-QA)(gly)]	1st	–	–	–	–	–	–	–	–
	2nd	2.00	0.996	90.8	81.6	2.00	0.997	92.90	80.2
	3rd	0.00	0.994	182	171	0.00	0.999	189.9	175.6

Activation energies, E_1 at 10^4 Gy, E_2 at 10^5 Gy, kJ mol^{-1}

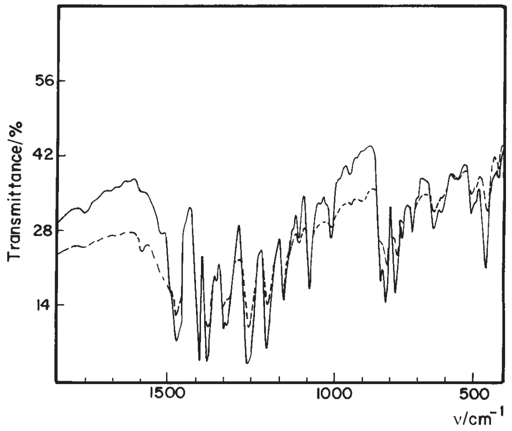

Fig. 5 IR spectra of unirradiated (—) and γ-irradiated (----) [Co(p-Me-QA)(gly)]. Irradiation dose=1·10^5 Gy

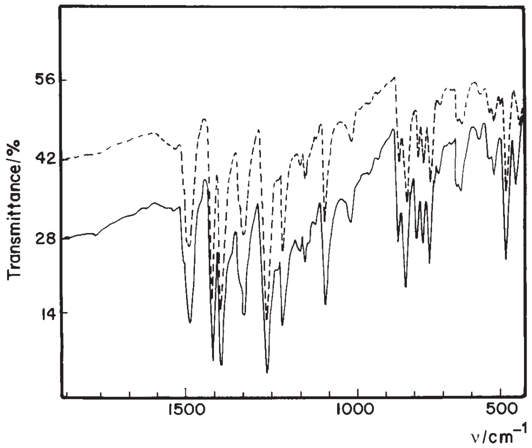

Fig. 6 IR spectra of unirradiated (—) and γ-irradiated (----) [Cu(p-Me-QA)(gly)]. Irradiation dose=1·10^5 Gy

Cu(II) show some inhibiting activity against them. It is thought [22] that the increase in the activity of the complexes may be due to the effect of metal ions on the cell.

Conclusions

The thermoanalytical results of the Co(II), Ni(II) and Cu(II) complexes conclusively prove that the main feature of first step decomposition is the evolution of nitrogen and that the metal oxides CoO, NiO and CuO are the final products. The TG curves as well as the activation energies of decomposition for the Co(II) and Cu(II) complexes are more

Table 8 Antibacterial activity of the complexes

Complex	Bacteria			Fungi			
	B. Cereus G+ve	*E. Coli* G–ve	*P. Aeruginosa* G–ve	*P. oxaliaum*	*A. niger*	*A. flavus*	*T. roseun*
[Co(*p*-Me-QA)(gly)]	+++	–	++	–	++	+	++
[Ni(QA)$_2$(Hmet)(H$_2$O)]	+	–	–	–	–	–	–
[Ni(*p*-Me-QA)$_2$(Hmet)(H$_2$O)]	++	–	–	–	–	–	–
[Cu(*p*-Me-QA)(ala)]	+++	++	+	++	+++	++	++++

affected by γ-irradiation than those of Ni(II), indicating their lower stability and the autocatalytic effect of Co(II) and Cu(II) on the decomposition of these complexes.

References

1 A Kaiser, A. Longmann and P. Zeller, Experimentia, 120 (1964) 503.
2 C. E. Cerniglia, J. P. Freeman, W. Franklin and L. D. Pack, Carcinogenesis (London), 3 (1982) 1255.
3 S. Pati ‘The Chemistry of Hydrazo, Azo and Azoxy Groups’ Part 1, Wiley, New York 1975.
4 I. M. A. Awad, Phosphors, Sulfur and Silicon, 114 (1996) 17.
5 I. M. A. Awad, J. Chem. Tech. Biotechnol., 53 (1992) 277.
6 G. D. Tiwari and M. N. Mishra, J. Ind. Chem. Soc., 59 (1982) 362.
7 F. Banati and R. Ugo, J. Organometal. Chem., 10 (1967) 257.
8 A. S. A. Zidan, Synth. React. Inorg. Met.-Org. Chem., 24 (1994) 277.
9 A. H. Osman, A. S. A. Zidan, A. I. El-Said and A. A. M. Aly, Transition Met. Chem., 18 (1993) 34.
10 P. Indrasenan and M. Lakshmy, Indian J. Chem., 36A (1997) 998.
11 M. Gupta and M. N. Srivastava, Synth. React. Inorg. Met.-Org. Chem., 26 (1996) 305.
12 V. K. Saxena, M. Gupta and M. N. Srivastava, Synth. React. Inorg. Met.-Org. Chem., 26 (1996) 1661.
13 B. V. Murdula, G. Venkertanarayana and P. Lingaiah, Indian J. Chem., 28A (1989) 104.
14 M. Gupta and M. N. Srivastava, Polyhedron, 4 (1985) 475.
15 B. T. Khan, K. Najmuddin, S. Shamsuddin and S. M. Zakeruddin, Inorg. Chim. Acta, 57 (1990) 175.
16 A. B. Akbarov and A. S. Mutalibov, Deposited Doc., 14 (1984) 685.
17 H. Rau, Angew. Chem. Internat. Edit. Eng., 12 (1973) 224.
18 I. M. A. Awad, A. A. M. Aly, A. A. Badel Hafez and Kh. M. Hassan, J. Chim. Chem. Soc., 36 (1989) 170.
19 A. W. Coats and J. P. Redfern, Nature, 20 (1964) 68.
20 H. H. Horowitz and G. Metzger, Anal. Chem., 35 (1963) 1464.
21 R. M. Mahfowz, A. A. M. Aly, M. S. El-Meligy and A. S. A. Zidan, Isotopen praxis, 27 (1991) 245.
22 R. Malhotra, J. P. Singh, M. Dudeja and K. S. Dhindsa, J. Inorg. Biochem., 46 (1992) 119.